The International Journal of Engineering and Science (IJES)
|| Volume || 13 || Issue || 1 || Pages || PP 35-43 || 2024 ||
ISSN (e): 2319 – 1813 ISSN (p): 2319 – 1805

Study on Electroosmotic Transport of Peristaltic Flow in Microchannel

Dibjyoti Mondal[1] and Mithilesh Kumar Chaube[2]
[1]*Discipline of Mathematics, National Institute of Technology Tiruchirappalli, Tamilnadu, India*
[2]*Discipline of Mathematics, Dr. S.P. Mukherjee International Institute of Information Technology Naya Raipur, Chhattisgarh, India*

---***ABSTRACT***---
In this paper, the peristaltic transport of electroosmotic fluid flow is discussed. A model for transporting a fluid bolus along the channel length is established by the presence of a non-integral number of waves propagating in the channel. An appropriate perturbation technique is applied for the analytical solution. To simplify the fluid mechanics analysis in capillary electrophoresis, the electrical double layer (EDL) at the surface of the capillary wall is assumed to be extremely thin. The electroosmotic slip velocity at the wall is used to approximate the impact of the applied electric field on the fluid velocity.

KEYWORDS:- *Peristaltic flow, Electric field, Perturbation Method, Electroosmotic slip velocity, EDL.*

Date of Submission: 02-01-2024 Date of acceptance: 14-01-2024

I. INTRODUCTION

Electroosmotic transport has essential applications in various fields, including microfluidics, electrokinetic, and chemical analysis. An electric field can cause fluid to move, a phenomenon known as electroosmotic transport. Peristaltic flow is a particular kind of fluid motion that happens when a fluid is forced to move through a tube or channel by a sequence of contractions and relaxations of the tube or channel walls. There are several real-world applications for peristaltic flow, including peristaltic pumps used in industrial, medical, and food processing activities. Combining electroosmotic transport and peristaltic flow has several advantages over traditional fluid pumping mechanisms. Fung and Yih [1] presented a theoretical analysis of the dynamics of peristaltic transport and discussed its applications in various biological systems. Misra and Pandey [2] provided valuable insights into the complex dynamics of blood flow in microvessels and highlighted the potential role of peristalsis in regulating blood flow and oxygen delivery. In [3], Chu and Fang described the flow of a Newtonian fluid in a two-dimensional channel with an elastic wall that undergoes sinusoidal peristaltic motion using a mathematical model based on the Navier-Stokes equations and the slip boundary condition. Siklauri and Beresnev [4] investigated the consequences of non Newtonian behavior on peristaltic flow in a tube filled with a Maxwell fluid. Also, Peristaltic transport is being explored by a group of researchers listed in references [5, 6, 7, 8]. Furthermore, Abd-Alla et al. [9] examined the movement of a Jeffrey fluid in a channel using peristaltic motion, considering the impact of both a magnetic field and gravity. The recent work of Vijayakumar and Reddy [10] contributed to the study of non-Newtonian fluid peristaltic transport. Their analysis of the flow behavior in the context of suction and injection can help to understand and optimize many critical industrial and physiological processes.

Understanding fundamental fluid dynamics, creating effective microfluidic systems, and creating new applications in biomedical engineering and environmental engineering all depend on the research of electroosmotic transport of peristaltic flow. Electroosmotic transport refers to the movement of fluids through a channel propelled by an electric field. The zeta potential represents a crucial parameter that affects the electroosmotic transport through the channel. The Helmholtz Smoluchowski equation [11] can be used to describe the electroosmotic transport in a channel with small zeta potentials. This equation relates the electroosmotic flow velocity to the zeta potential, the permittivity of the fluid, the viscosity of

the fluid, and the applied electric field. Dutta [12] discussed the phenomenon of electroosmotic transport, which is the motion of a fluid caused by an applied electric field in a charged porous medium. Chakraborty [13] demonstrated the correlation between the electroosmotic and peristaltic mechanisms. Later, Tripathi [14] analyzed the electrokinetic transport of aqueous electrolyte fluid with a Newtonian model in the presence of peristaltic through the microchannel. To make the problem simpler, he applied Debye-Huckel linearization and employed the electroosmotic slip velocity at the wall as a boundary condition. Guo and Qi [15] presented a theoretical analysis of the electroosmotic peristalsis of a fractional Jeffreys fluid in a microchannel. Kiran et al. [7] provided a theoretical frame work for understanding the complex fluid dynamics and chemical reactions in the digestive process. It highlighted the importance of considering the coupling between fluid mechanics and chemical kinetics in such systems. Moreover, Tripathi et al.[16] developed a hydrodynamics model to examine the impact of the electric double layer's thickness and the external electric field on the peristaltic pumping of viscous fluids within a microchannel. See [17, 18, 19] for a recent review of this topic.

Motivated by the studies mentioned earlier, the aim is to study how the Helmholtz-Smoluchowski velocity affects peristaltic flow in a microchannel, as well as to explore the role of electrokinetic transport in peristaltic pumping. Non integral fluid boluses are assumed to flow down the channel, and the electrical double layer (EDL) is treated very thin for simplicity's sake. The effect of the applied electric field on the channel wall is described using the electroosmotic slip velocity at the wall, and a perturbation method is employed. Additionally, the mean axial velocity is calculated for the free-pumping case.

The mathematical formulation and solutions of the considered problems are presented in Section II and Section III, respectively. In Section IV, the results are discussed in detail. Finally, conclusions are drawn in Section V.

II MATHEMATICAL MODEL

Consider a two-dimensional flow that is unsteady, viscous, and incompressible while being subject to an electrokinetic body force applied axially. Then, the equations of motion are given as [14]

$$\rho\left(\frac{\partial u}{\partial t}+u\frac{\partial u}{\partial x}+v\frac{\partial u}{\partial y}\right)=-\frac{\partial p}{\partial x}+\mu\nabla^2 u+\rho_e E, \tag{1}$$

$$\rho\left(\frac{\partial v}{\partial t}+u\frac{\partial v}{\partial x}+v\frac{\partial v}{\partial y}\right)=-\frac{\partial p}{\partial y}+\mu\nabla^2 v, \tag{2}$$

and

$$\frac{\partial \mathrm{u}}{\partial \mathrm{x}}+\frac{\partial \mathrm{v}}{\partial \mathrm{y}}=0, \tag{3}$$

where ρ stands for fluid density, u and v represent the velocity components, p signifies pressure, μ denotes viscosity, and E symbolizes the electric field, and ∇^2 is the Laplacian operator. Here ρ_e is electric charge density which is defined as [14]

$$\rho_e=-2n_0 ez\left(\frac{ze\phi}{K_B T}\right), \tag{4}$$

where n_0 is concentration of ions at the bulk, e be the charge of electron, z is charge balance, K_B be Boltzmann constant, T represents the temperature and ϕ represents electric potential function. The expression for the Poisson-Boltzmann equation takes the form of

$$\nabla^2\phi=-\frac{\rho_e}{\epsilon_1}. \tag{5}$$

Here, ϵ_1 refer to the permittivity.

Let η be vertical wall displacement, defined as [1], $\eta=a\cos\frac{2\pi}{\lambda}(x-ct)$. Here, a is the wave'samplitude, λ is the wavelength, and c is the wave speed; see Figure 1. Now we are applying the following non-dimensional form [1]

$$x' = \frac{x}{d}, \quad y' = \frac{y}{d}, \quad u' = \frac{u}{c}, v' = \frac{v}{d}, \ \eta' = \frac{\eta}{d},$$
$$p' = \frac{p}{\rho c^2}, \quad \phi' = \frac{\phi}{\zeta}, \ \epsilon = \frac{a}{d}, \alpha = \frac{2\pi d}{\lambda}, \quad R = \frac{c d}{\lambda}. \tag{6}$$

Here, ϵ denotes the ratio of amplitudes, a signifies the wave number, R stands for the Reynolds number, ζ represents the zeta potential, and d indicates half of the average space between the

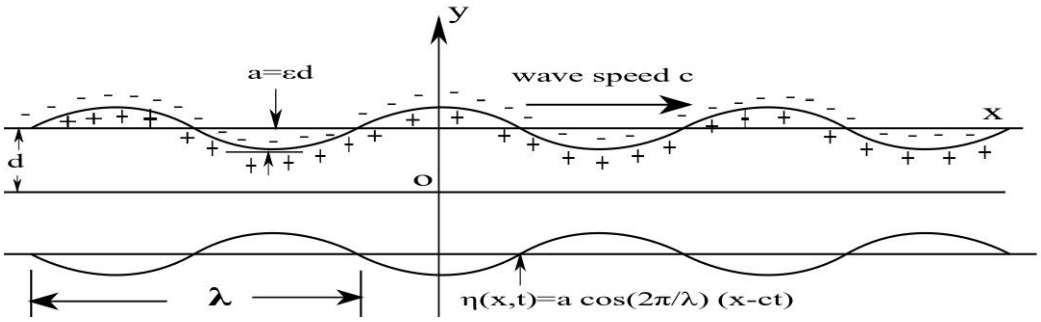

Figure1: Schematic diagram of physical problem

boundaries. After using the non-dimensional parameter as in (6) and using the equations (4)-(5), we get the dimensionless form of (1)-(3)

$$R\left(\frac{\partial u}{\partial t} + u\,\frac{\partial u}{\partial x} + v\,\frac{\partial u}{\partial y}\right) = -R\,\frac{\partial p}{\partial x} + \nabla^2 u + m^2 U_{HS}\phi, \tag{7}$$

$$R\left(\frac{\partial v}{\partial t} + u\,\frac{\partial v}{\partial x} + v\,\frac{\partial v}{\partial y}\right) = -R\,\frac{\partial p}{\partial x} + \nabla^2 v, \tag{8}$$

$$\frac{\partial u}{\partial x} + \frac{\partial v}{\partial y} = 0, \tag{9}$$

where $U_{HS} = -\frac{E\epsilon_1\zeta}{\mu c}$, represents Helmholtz-Smoluchowski velocity and $m = aez\sqrt{\frac{2n_0}{\epsilon_1 K_B T}}$ represents electroosmotic parameter. The momentum equation for a thin electric double layer (EDL) may exclude the electrokinetic body force term [14]. Then, from(7)-(9), we have

$$R\left(\frac{\partial u}{\partial t} + u\,\frac{\partial u}{\partial x} + v\,\frac{\partial u}{\partial y}\right) = -R\,\frac{\partial p}{\partial x} + \nabla^2 u, \tag{10}$$

$$R\left(\frac{\partial v}{\partial t} + u\,\frac{\partial v}{\partial x} + v\,\frac{\partial v}{\partial y}\right) = -R\,\frac{\partial p}{\partial x} + \nabla^2 v, \tag{11}$$

$$\frac{\partial u}{\partial x} + \frac{\partial v}{\partial y} = 0, \tag{12}$$

After eliminating the pressure term from (10) and (11), the resulting equation becomes

$$\frac{\partial}{\partial t}\nabla^2\psi + \psi_y\nabla^2\psi_x - \psi_x\nabla^2\psi_y = \frac{1}{R}\nabla^2\nabla^2\psi, \tag{13}$$

where ψ be stream function, defined as $u = \frac{\partial\psi}{\partial y}$ and $v = -\frac{\partial\psi}{\partial x}$, and ψ_x and ψ_y are partial derivative of ψ with respect to x and y, respectively. Now, the boundary conditions are written as

$$u = \psi_y = U_{HS} \text{ and } v = \psi_x = \mp\alpha\epsilon \sin\alpha(x - t), \tag{14}$$

when $y = \pm(1 + \eta)$.

III SOLUTION PROCEDURE

Consider ψ and $\frac{\partial p}{\partial x}$ as [1]

$$\psi = \psi_0 + \epsilon\psi_1 + \epsilon^2\psi_2 + \ldots, \tag{15}$$

$$\frac{\partial p}{\partial x} = \left(\frac{\partial p}{\partial x}\right)_0 + \epsilon\left(\frac{\partial p}{\partial x}\right)_1 + \epsilon^2\left(\frac{\partial p}{\partial x}\right)_2 + \ldots. \tag{16}$$

Substituting (15) into (13) and equating the coefficient of ϵ, and also neglecting the higher term after the square of ϵ, we get

$$\frac{1}{R}\nabla^2\nabla^2\psi_0 = \frac{\partial}{\partial t}\nabla^2\psi_0 + \psi_{0_x}\nabla^2\psi_{0_x} - \psi_{0_x}\nabla^2\psi_{0_y}, \tag{17}$$

$$\frac{1}{R}\nabla^2\nabla^2\psi_1 = \frac{\partial}{\partial t}\nabla^2\psi_1 + \psi_{0_y}\nabla^2\psi_{1_x} + \psi_{1_y}\nabla^2\psi_{0_x} - \psi_{0_x}\nabla^2\psi_{1_y} - \psi_{1_x}\nabla^2\psi_{0_y}, \tag{18}$$

$$\frac{1}{R}\nabla^2\nabla^2\psi_2 = \frac{\partial}{\partial t}\nabla^2\psi_2 + \psi_{0_y}\nabla^2\psi_{2_x} + \psi_{1_y}\nabla^2\psi_{1_x} + \psi_{2_y}\nabla^2\psi_{0_x} - \psi_{0_x}\nabla^2\psi_{2_y} - \psi_{1_x}\nabla^2\psi_{1_y} - \psi_{2_x}\nabla^2\psi_{0_y}. \tag{19}$$

Also, by substituting (15) into (14), we get the boundary conditions

$$\psi_{0_y}(\pm 1) = U_{HS}, \tag{20}$$

$$\psi_{1_y}(\pm 1) \pm \psi_{0_{yy}}(\pm 1)\cos\alpha(x - t) = 0, \tag{21}$$

$$\psi_{2_y}(\pm 1) \pm \psi_{1_{yy}}(\pm 1)\cos\alpha(x - t) + \frac{1}{2}\psi_{0_{yyy}}(\pm 1)\cos^2\alpha(x - t) = 0, \tag{22}$$

and

$$\psi_{0_x}(\pm 1) = 0, \tag{23}$$

$$\psi_{1_x}(\pm 1) \pm \psi_{0_{xy}}(\pm 1)\cos\alpha(x - t) = \mp\alpha\sin\alpha(x - t), \tag{24}$$

$$\psi_{2_x}(\pm 1) \pm \psi_{1_{xy}}(\pm 1)\cos\alpha(x - t) + \frac{1}{2}\psi_{0_{xyy}}(\pm 1)\cos^2\alpha(x - t) = 0, \tag{25}$$

Under the following two conditions [1] (a) the flow exhibits symmetry, and (b) there is a uniform pressure gradient along the x axis, from (17), (20), and (23), the solution leads to the standard Poiseuille flow equation

$$\psi_0 = K\left(y - \frac{y^3}{3}\right) + U_{HS}y, \tag{26}$$

where

$$K = -\frac{R}{2}\left(\frac{\partial p}{\partial x}\right)_0. \tag{27}$$

Now assume that the solutions of equations (18), (21), and (24) and equations (19), (22), and (25) are [1]

$$2\psi_1 = \Phi_1(y)e^{-i\alpha(t-x)} + \Phi_1^*(y)e^{i\alpha(t-x)}, \tag{28}$$

and

$$2\psi_2 = \Phi_{20}(y) + \Phi_{22}(y)e^{-i2\alpha(t-x)} + \Phi_{22}^*(y)e^{i2\alpha(t-x)}, \tag{29}$$

respectively, where the asterisk indicates the complex conjugate. After putting (28) and (29) into equations (18), (19), (21), (22), (24), and (25), we get

$$\left(\frac{d^2}{dy^2} - \alpha^2 + i\alpha R[1 - U_{HS} - K(1-y^2)]\right) \times \left(\frac{d^2}{dy^2} - \alpha^2\right)\Phi_1 - i2K\alpha R\,\Phi_1 = 0, \tag{30}$$

with

$$\phi_1'(\pm 1) - 2K = 0, \tag{31}$$

$$\phi_1(\pm 1) = \pm 1, \tag{32}$$

and

$$\Phi_{20}'''' = -\frac{i\alpha \mathrm{R}}{2}(\Phi_1\Phi_1^{*\prime\prime\prime} - \Phi_1^*\Phi_1'')' \tag{33}$$

$$\left(\frac{d^2}{d\,y^2} - 4\,\alpha^2\right)\left[\frac{d^2}{d\,y^2} - (4\,\alpha^2 - 2\,i\,\alpha\,R)\right]\Phi_{22} = i\,2\,\alpha\,RK\,\left((1-y^2) + U_{HS}\right)$$

$$\left(\frac{d^2}{d\,y^2} - 4\,\alpha^2\right)\,\Phi_{22} + i\,4\,\alpha\,R\,K\,\Phi_{22} + \frac{i\,\alpha\,R}{2}(\Phi_1'\,\Phi_1'' - \Phi_1\,\Phi_1'''), \tag{34}$$

with

$$\Phi_{20}'(\pm 1) - 2K \pm \frac{1}{2}\left[\Phi_1''(\pm 1) + \Phi_1''(\pm 1)\right] = 0, \tag{35}$$

$$\Phi_{22}'(\pm 1) \pm \frac{1}{2}\Phi_1''(\pm 1) - \frac{K}{2} = 0, \tag{36}$$

$$\Phi_2(\pm 1) \pm \frac{1}{4}\Phi_1' = 0, \tag{37}$$

Now we consider that the pumping is free [1], which means that the pressure gradient at the boundary is zero i.e., $\left(\frac{\partial p}{\partial x}\right)_0$=0. Under this assumption, the coefficient K in the fourth-order differential equation that describes the flow can be set to zero, which simplifies the equation considerably. This is because K represents the resistance to the bending of the fluid streamlines, and when there is no pressure gradient at the boundary, there is no bending of the streamlines. Now, the solution of (30) with (31)-(32) is found as [1]

$$\Phi_1(y) = A\sinh\alpha y + B\sinh\beta y, \tag{38}$$

in which

$$A = \frac{-\beta\cosh\beta}{\alpha\sinh\beta\cosh\alpha - \beta\sinh\alpha\cosh\beta}, \tag{39}$$

$$B = \frac{\alpha\cosh\alpha}{\alpha\sinh\beta\cosh\alpha - \beta\sinh\alpha\cosh\beta}, \tag{40}$$

where

$$\beta^2 = \alpha^2 - i\alpha R(1 - U_{HS}). \tag{41}$$

Now, for determining the mean flow, substituting (38) into (33) and after integrating once, we get

$$\Phi_{20}''' = \frac{\alpha^2 R^2}{2}[A^* B \sinh\alpha\, y \sinh\beta\, y + AB^* \sinh\alpha\, y \sinh\beta^* y + 2B\,B^* \sinh\beta\, y \sinh\beta^* y] + 2C_1, \tag{42}$$

$$\Phi_{20}'(\pm 1) = \frac{1}{2}[(A + A^*)\alpha^2 \sinh\alpha + B\beta^2 \sinh\beta + B^*\beta^{*2} \sin\beta^*] \equiv D, \tag{43}$$

where C_1, D are constants. An integration of (42) yields the result

$$\Phi_{20}'(y) = F(y) + C_1 y^2 + C_2 y + C_3, \tag{44}$$

where C_2, C_3 are constants for integration and $F(y)$ is defined as

$$F(y) = \frac{\alpha^2 R^2}{2}\left\{\frac{A^* B}{2}\left[\frac{\cosh(\alpha+\beta)y}{(\alpha+\beta)^2} - \frac{\cosh(\alpha-\beta)y}{(\alpha-\beta)^2}\right] + \frac{AB^*}{2}\left[\frac{\cosh(\alpha+\beta^*)y}{(\alpha+\beta^*)^2} - \frac{\cosh(\alpha-\beta^*)y}{(\alpha-\beta^*)^2}\right] + BB^*\left[\frac{\cosh(\beta+\beta^*)y}{(\beta+\beta^*)^2} - \frac{\cosh(\beta-\beta^*)y}{(\beta-\beta^*)^2}\right]\right\}. \tag{45}$$

By using (43), we can say that both C_1 and the mean pressure gradient $\overline{\frac{\partial p}{\partial x}}$ are proportional, and it can be written as [1]

$$\overline{\frac{\partial p}{\partial x}} = \overline{\epsilon^2\left(\frac{\partial p}{\partial x}\right)_2} = \frac{\epsilon^2}{2\mathrm{R}}\Phi_{20}''' + \frac{\epsilon^2}{4} i\alpha(\Phi_1\Phi_1^{*\prime\prime} - \Phi_1^*\Phi_1'') + O(\epsilon^3),$$
$$= \frac{\epsilon^2}{R} C_1 + O(\epsilon^3), \tag{46}$$

i.e.

$$\overline{\left(\frac{\partial p}{\partial x}\right)_2} = \frac{C_1}{R}. \tag{47}$$

Now, we can express the average velocity in the axial direction [1]

$$\overline{u} = \frac{\epsilon^2}{2}\Phi_{20}' = \frac{\epsilon^2}{2}[D + F(y) - C_1(1 - y^2) - F(1)]. \tag{48}$$

Now, using (47), it can be written as

$$\overline{u} = \frac{\epsilon^2}{2}\left[D + F(y) - R\,\overline{\left(\frac{\partial p}{\partial x}\right)_2}(1 - y^2) - F(1)\right]. \tag{49}$$

We define

$$G(y) = \frac{200}{\alpha^2 R^2}[F(1) - F(y)]. \tag{50}$$

Since on the centreline, the mean velocity to be zero is the condition of critical reflux. Therefore, mathematically, it can be written as

$$\overline{\left(\frac{\partial p}{\partial x}\right)}_{2\ \text{critical reflux}} = \frac{1}{R}\left[D - \frac{\alpha^2 R^2}{200} G(0)\right]. \tag{51}$$

IV RESULTS AND DISCUSSION

In the preceding section, we computed the time-averaged velocity and the critical pressure for reflux. This section will look into the problem and create a graph for the quantities, as mentioned earlier.

From Figure 2 and Figure 3, we have seen that the flow and wave amplitude ratio depend on each other very strongly. When the amplitude ratio increases, the mean axial velocity also increases, and the flow changes very close to the boundary since the amplitude ratio takes higher values. Figure 4 and Figure 5 agree with the reported results of [1]. This represents that the said critical reflux is reduced with the rise in Reynolds numbers. Figure 6 shows the effect of the external electric field in the variation of mean axial velocity against the transverse displacement at constant values of $\alpha = 0.25$, $\epsilon = 0.5$, and $R = 15$. We noticed that the velocity profile increases with an added electric field while decreasing with an opposing electric field. So, we can say that the mean axial velocity may be controlled by using electric chips.

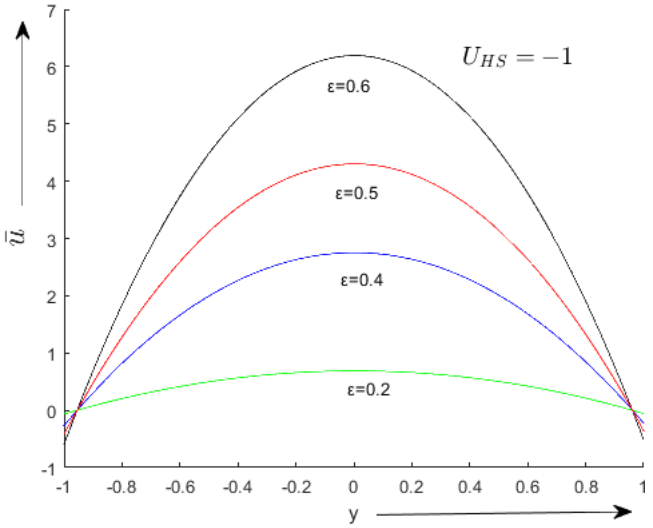

Figure2:Mean velocity in axial direction vs. displacement for various value of amplitude ratio (ϵ), $\overline{\left(\frac{\partial p}{\partial x}\right)}_2 = 2.5$ and $U_{Hs} = -1$.

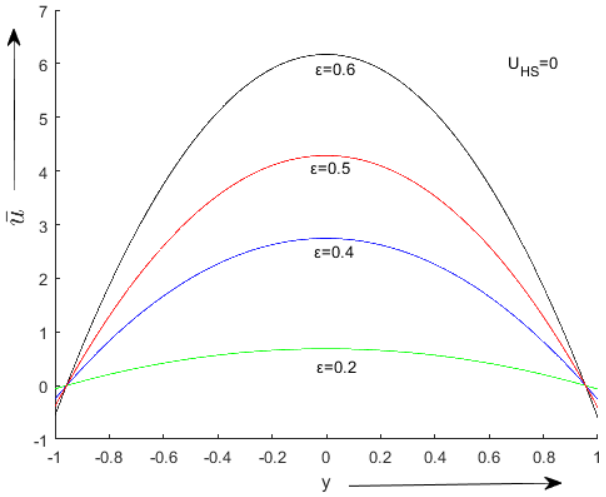

Figure3:Mean velocity in axial direction vs. displacement for various value of amplitude ratio (ϵ), $\overline{\left(\frac{\partial p}{\partial x}\right)}_2 = 2.5$ and $U_{Hs} = 0$.

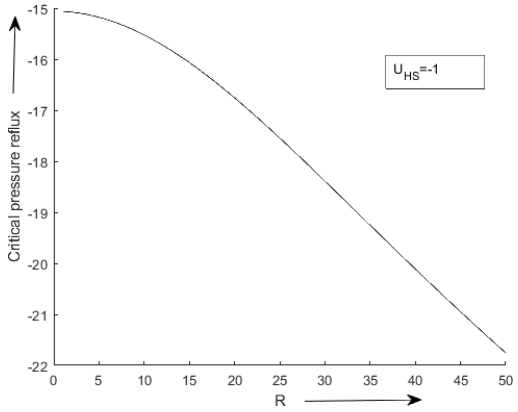

Figure 4: Critical pressure for reflux vs. Reynolds number for $\overline{\left(\frac{\partial p}{\partial x}\right)}_{2\text{ critical reflux}}$, $\alpha = 0.2$ and $U_{HS} = -1$.

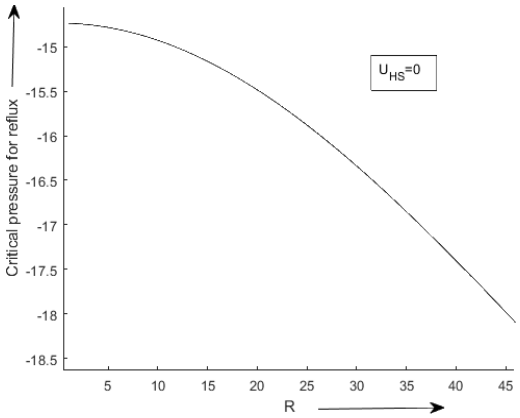

Figure 5: Critical pressure for reflux vs. Reynolds number for $\overline{\left(\frac{\partial p}{\partial x}\right)}_{2\text{ critical reflux}}$, $\alpha = 0.2$ and $U_{HS} = 0$.

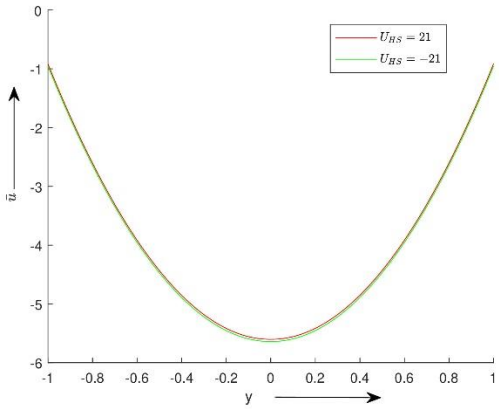

Figure 6: Mean axial velocity vs. transverse displacement for various Helmholtz-Smoluchowski velocity values at constant values α=0.25, ϵ=0.5, R=15 and $\overline{\left(\frac{\partial p}{\partial x}\right)}_2 = 2.5$.

V CONCLUSIONS

A few key results of the study are outlined below

- For any value of Helmholtz-Smoluchowski velocity, the mean axial velocity is proportional to the amplitude ratio squared.
- The wave's amplitude ratio has a significant impact on the flow.
- When the amplitude ratio increases, the mean axial velocity also increases.
- For any value of Helmholtz Smoluchowski velocity, the rise of Reynolds numbers, the said critical reflux is reduced.
- An applied electric field may control mean axial velocity.
- This model may be generalized for flow and non-Newtonian fluid types.

REFERENCES

[1] YCFungandCSYih. Peristaltictransport.*JournalofAppliedMechanics*,1968.

[2] JCMisraandSKPandey.Peristalticttransportofbloodinsmallvessels:studyofamathematical model.*Computers & Mathematics with Applications*,43(8-9):1183–1193,2002.

[3] W Chu and J Fang.Peristaltic transport in a slip flow.*The European Physical JournalB-CondensedMatterandComplexSystems*,16(3):543–547,2000.

[4] DavidTsiklauriandIgorBeresnev.Non-newtonianeffectsintheperistalticflowof amaxwellfluid.*PhysicalReviewE*,64(3):036303,2001.

[5] Noreen Sher Akbar and S Nadeem. Peristaltic flow of a micropolar fluid with nano particlesinsmallintestine.*AppliedNanoscience*,3(6):461–468,2013.

[6] GC Shit and M Roy. Effect of slip velocity on peristaltic transport of a magneto-micropolarfluid through a porous non-uniform channel. *International Journal of Applied and Compu-tationalMathematics*,1(1):121–141,2015.

[7] GRaviKiran,GRadhakrishnamacharya,andOAnwarBég.Peristalticflowandhydrody-namicdispersionofareactivemicropolarfluid-simulationofchemicaleffectsinthedigestiveprocess.*JournalofMechanicsinMedicineandBiology*,17(01):1750013,2017.

[8] Sanjay Kumar Pandey and Dharmendra Tripathi.Unsteady peristaltic flow of micro-polarfluidinafinitechannel.*ZeitschriftfürNaturforschungA*,66(3-4):181–192,2011.

[9] AMAbd-Alla,SMAbo-Dahab,andMaramMAlbalawi.Magneticfieldandgravityeffectson peristaltic transport of a jeffrey fluid in an asymmetric channel.*Abstract and AppliedAnalysis*,2014.

[10] P Vijayakumar and R Hemadri Reddy. An effective analysis of non-newtonian fluid peri-staltic transport in recent developments with suction and injection through channels. *Jour-nalofXidianUniversity*,2023.

[11] StaffanWall.Thehistoryofelectrokineticphenomena.*CurrentOpinioninColloid &InterfaceScience*,15(3):119–124,2010.

[12] Debashis Dutta.Electroosmotic transport through rectangular channels with small zetapotentials.*Journalofcolloidandinterfacescience*,315(2):740–746,2007.

[13] Suman Chakraborty. Augmentation of peristaltic microflows through electro-osmotic mech-anisms.*JournalofPhysicsD:AppliedPhysics*,39(24):5356,2006.

[14] DharmendraTripathi,JanakMulchandani,andShubhamJhalani.Electrokinetictransportin unsteady flow through peristaltic microchannel. In *AIP Conference Proceedings*, volume1724,page020043.AIPPublishingLLC,2016.

[15] Xiaoyi Guo and Haitao Qi.Analytical solution of electro-osmotic peristalsis of fractionaljeffreysfluidinamicro-channel.*Micromachines*,8(12):341,2017.

[16] DTripathi,ShashiBhushan,AshuYadav,andAshishSharma.Mathematicalstudyofperistalsis in the presence of electrokinetic transport in parallel plate microchannel.In*ApplicationsofFluidDynamics*,pages273–281.Springer,2018.

[17] K Ramesh,DTripathi,MMBhatti,andCMKhalique.Electro-osmoticflowofhydro-magnetic dusty viscoelastic fluids in a microchannel propagated by peristalsis.*Journal ofMolecularLiquids*,314:113568,2020.

[18] Choudhari Rajashekhar, Fateh Mebarek-Oudina, Ioannis E Sarris, Hanumesh Vaidya, Kere-halli V Prasad, Gudekote Manjunatha, and Hadimane Balachandra. Impact of electroos-mosis and wall properties in modelling peristaltic mechanism of a jeffrey liquid through amicrochannelwithvariablefluidproperties.*Inventions*,6(4):73,2021.

[19] T Salahuddin, Iqra Kousar, and Mair Khan.Electrokinetically driven peristaltic flow ofnanofluid in a curved microchannel. *Materials Science and Engineering: B*, 284:115886,2022.